Radar phase based near surface meteorological data retrievals

Author: Josep Ruiz Rodon

Advisor: Joan Bech Rustullet

Facultat de Física, Universitat de Barcelona, Diagonal 645, 08028 Barcelona, Spain*.

Abstract: The aim of this project is to analyze the relation between the meteorological changes in the tropospheric layer and the signal phase history from radar acquisitions. Atmospheric temperature, pressure and relative humidity impact on the atmospheric refraction index is stated which, at the same time, has a critical impact on the radar phase signal. Data from radar GB-SAR campaigns are used to demonstrate the theoretical relation.

I. INTRODUCTION

Radar imaging is an extended remote sensing technique which is intended to get 2D images. Radar is an active remote sensing technique which illuminates the target scene with its own generated signal and collects and processes echoes coming from targets. So, each pixel of the image contains the information of radar backscatter [1] (amplitude and phase) of a particular region of the scene. In radar, the time delay of the different echoes received is necessary to locate the position of the targets in the scene. The time taken by electromagnetic waves to reach a target at range (R) and return is

$$t = 2R\frac{n}{c}, \tag{1}$$

where c is the speed of light in vacuum and n the air refraction index. As seen, (1) has two unknowns, the range and the refractivity index. However, from the point of view of most of the radar's applications, the refraction index varies by at most 0.03% and it can be considered constant for the entire travel path.

The basic idea to extract the information of the refraction index from radar measurements is to think the other way around. So, if a fixed target is considered within the illuminated scene by the radar, the range between the radar and this target is kept constant during the whole data acquisition. Thus, in that case, the changes observed in the travel time can be directly related to changes in the refraction index along the signal path.

Some limitations to retrieve the refraction index information are the accuracy required in the time echo return calculation and the precision of the distance between the radar and the target of interest. The second case is a minor problem because, if we are able to determine the range to a fixed target with a fair precision, we still can relate changes in travel time to changes in the refraction index. However, the absolute calibration would then be performed by other means. On the other hand, the accuracy on the time travel determination problem can be solved by using the phase differences of the received signals. The magnitude of the phase change ($\Delta\varphi$) is a linear function of the travel time of the electromagnetic phase and can be related to the refraction index as,

$$\Delta\varphi = 2\pi f \Delta t = \frac{4\pi f R}{c}\Delta n \tag{2}$$

being f the radar transmitted frequency. Thus, the phase differences are the result of the changes in the refractive index within the travel path. Thus, by measuring the phase changes along time, the refraction index can be derived.

II. IMPACT OF METEOROLOGICAL DATA ON REFRACTION INDEX AND RADAR PHASE

Once the index of refraction impact on the phase shift in the radar signal has been established, the relation with meteorological data is studied. It is common to express the index of refraction in terms of the refractivity (N) which is defined as the amount that the index of refraction exceeds the value in vacuum in parts per million:

$$N = (n-1) \times 10^6 \ . \tag{3}$$

On the other hand, the refractivity can be directly related with meteorological magnitudes such as pressure, temperature and moisture as [2]

$$N = 77.6\frac{P}{T} + 3.73 \times 10^5 \frac{e}{T^2} \ , \tag{4}$$

being P the air pressure [hPa], T the temperature [K] and e the water vapour pressure [hPa]. The water vapour pressure can be related with the relative humidity (RH) as

$$e = \frac{6.11}{100} RH(\%) \cdot 10^{\frac{7.5 \cdot T(°C)}{237.3 + T(°C)}} \ . \tag{5}$$

The two terms that compose equation (4) are known as a density term and an additional wet term. The wet term is the one that makes the refractivity dependant on the air moisture.

At low temperature the moisture is low and the index of refraction depends mostly on the temperature. As the temperature gets higher, the quantity of moisture that the air can hold increases significantly and, thus, the additional wet term impact on the refractivity becomes more important. So, at higher temperature, the index of refraction becomes more sensitive to changes in moisture than to changes in temperature.

A. Index of refraction variations.

Let us consider the total derivative of the refractivity given by the equation (4),

$$dN = \frac{\partial N}{\partial P}dP + \frac{\partial N}{\partial T}dT + \frac{\partial N}{\partial e}de \tag{6}$$

where the partial derivatives with respect to pressure, temperature and water vapour pressure can be computed as

$$\frac{\partial N}{\partial P} = \frac{77.6}{T} \tag{7}$$

---

* Electronic address: `jruizrod13@alumnes.ub.edu`

$$\frac{\partial N}{\partial T} = -\left(77.6\frac{P}{T^2} + 7.46 \times 10^5 \frac{e}{T^3}\right) \qquad (8)$$

$$\frac{\partial N}{\partial e} = \frac{3.73 \times 10^5}{T^2} \qquad (9)$$

respectively. Thus, the impact on the radar signal phase can be obtained from (2):

$$\Delta\varphi = \frac{4\pi f R \cdot 10^{-6}}{c}\Delta N \quad, \qquad (10)$$

where the derivatives have been substituted by increments considering that temporal and spatial variations of the meteorological magnitudes will be smooth and slow.

So, the changes in the atmospheric conditions could be detected by measuring the phase changes received in the radar from stable targets. However, some limitation shall be considered. First, the presence of coherent targets [3] (stable intrinsic phase) is required. Otherwise, if non-stable targets are considered to retrieve the meteorological parameters, the own target phase variation will mask the actual changes on the atmospheric conditions. Examples of stable targets that one may find in a scene would be rocks, man-made structures (buildings, fences, etc.), communications antennas, electricity poles, etc. Examples of non-stable targets, which are known as clutter [4] in most of radar applications, will be forests in windy conditions, water surfaces, moving targets, etc. Second, the frequency stability of the radar [5] must be assured during the whole atmospheric monitoring. If frequency drifts are present in the radar system, it will be counted as atmospheric changes and it will blur our estimation of meteorological parameters evolution. However, current oscillators used in radar applications are stable enough for the purpose considered in this analysis.

The impact of the changes of the different meteorological magnitudes on the phase of the radar signal is studied separately.

Let us consider as a first approximation the impact of the pressure variations on the received signals taking the temperature and water vapour pressure as constant magnitudes (dT=de=0). Taking as an example an atmospheric pressure of 1000 hPa with a temperature of 300 K and 50% of relative humidity (which corresponds to a dew point of 289K and a water vapour pressure of 18 hPa), a change of 1 hPa in the pressure corresponds roughly to a change of 0.26 in the refractivity. Considering an X-band radar at 9.65 GHz and a range to the scene around 1 km, a radar signal phase of 5.96 deg·km^{-1}·hPa^{-1} is obtained.

These results show the feasibility of retrieving atmospheric pressure changes from the variations of the radar phase signal. However, some constraints shall be considered. The phase of any signal is a 2π rad periodic function and it can result in phase wrapping. So, if the phase changes more than 2π rad from one measurement to the other, the estimation may be incorrect. This implies that both large ranges (linear dependence between phase changes and range) and monitor changes in turbulent atmospheric scenarios should be avoided. Considering the previous example, taking a scene range of 20 km and a change on the atmospheric pressure of 3 hPa, it will result in a phase change around 360 degrees, which could be interpreted as no change at all,

giving a wrong estimation of the pressure evolution. Then, our analysis is centred in low-range applications (from 1 to 5 km at most) which will offer a large range of detectable changes of the atmospheric condition without phase wrapping. Additionally, there are several techniques to unwrap the radar phase signals that could be applied for retrieving the actual phase evolution of the signal [6].

Similarly, the impact of the temperature variations in the radar phase signal is analysed. In this case, the atmospheric pressure and water vapour pressure are considered invariant magnitudes (dP=de=0). Considering the same values than in the previous example (an atmospheric pressure of 1000 hPa with a temperature of 300 K and a water vapour pressure of 18 hPa), it results to a phase change of 31.33 deg·km^{-1}·K^{-1} considering a frequency of 9.65 GHz. If we limit the scene range to 2 km, the range of detectable temperature changes without phase wrapping will be around 4-5 ℃.

Finally, the water vapour pressure variations can also be related to the phase changes on the received radar signal. Considering atmospheric pressure and temperature as constants (dP=dT=0) and taking a temperature of 300 K, a phase variation of 237.2 deg·km^{-1}·hPa^{-1} is obtained (corresponding to a HR change from 50 to 54%). Therefore, this technique will be really accurate to detect small changes in the water vapour content of the atmosphere.

Additionally, the spatial change of temperature and atmospheric pressure over a large scene will be in general smooth, i.e. we do not see large temperature or pressure differences over a valley in a local scale (1 to 5 km). Therefore, apart from the temporal evolution of the water vapour pressure considering different radar acquisition along time, we may be capable of retrieving the spatial changes of this parameter if we have several coherent targets distributed all along the monitored scene. That makes this technique quite interesting for meteorological purposes since it can offer spatial-temporal information of the water vapour pressure which can be directly related to precipitation. Furthermore, the range limitations could be improved to tens of kilometres by considering an S-band radar (3 GHz).

B. Propagation delay over non-constant index of refraction

The meteorological conditions may change in the path from the radar to the target resulting in a space-time varying index of refraction. So, considering that the phase of the target is constant along time and the variations of the refraction index n(x,y,z,t), the phase drift from two different acquisitions is computed as

$$\Delta\varphi = \varphi(t_1) - \varphi(t_0) =$$

$$= \frac{4\pi f}{c}\int_0^r [n(x,y,z,t_1) - n(x,y,z,t_0)]dr' \qquad (11)$$

so, (11) accounts for changes in atmospheric pressure, temperature or water vapour along the signal path.

C. Measuring the field of refractive index in flat terrain. Differential phase changes

One of the limitations presented before is the phase wrapping where changes in phase of more than 2π radians

can be interpreted wrongly. This implies that there is an ambiguity in the phase measurement of a single target at a range of few tens of kilometres. Since the range between the radar and the scene is fixed by the acquisition scenario (radar placed at the top of a mountain, building), the solution relays on considering two different targets in the scene in the same direction and computing their phase changes independently, by using (11). Then, the difference between phase shifts from the two targets may be used to get the refraction index between these positions. The result will be

$$\Delta\varphi_{T1} - \Delta\varphi_{T2} = [\varphi(T2, t_1) - \varphi(T2, t_0)] -$$

$$-[\varphi(T1, t_1) - \varphi(T1, t_0)] \approx \qquad (12)$$

$$\approx \frac{4\pi f}{c} \int_{r(T1)}^{r(T2)} [n(r', t_1) - n(r', t_0)] dr'$$

where T1 and T2 stand for the target 1 and target 2. The advantage of using (12) with two targets close enough is that it will be difficult to have changes in the refraction index large enough to produce phase wrapping. The weak point of this approach is that the targets positions must be collinear and the terrain totally flat in order to have path overlapping to subtract one contribution from the other.

Another approach is to consider the targets temporal phase history. If consecutive acquisitions are taken, the changes in the refraction index from one to the other will be small enough to avoid phase wrapping, and get the temporal evolution of each point. Additionally, if several stable points in the scene are monitored, a spatial averaging can be applied over the scene to mitigate the target phase decorrelation.

D. Vertical structure of the refraction index

If we consider varying target heights, taking the phase difference between two separated targets method explained in the previous section is no longer applicable since the two paths do not overlap.

To account for the vertical structure of the refraction index one can use

$$n(x, y, z) \approx n(x, y, z_0) + (z - z_0)\left(\overline{\frac{dn}{dz}}\right) \quad . \qquad (13)$$

In this approach, the spatial variability of dn/dz is neglected over the area where the refraction index is computed. The calculation of the exact vertical component of the refraction index in each point may be complex and requires spatial interpolation (see for example [7]). Alternatively, triplets of close targets along a radial at different heights may be considered. If the same refractive index at the altitude of the radar is considered for all three, a system of two equations with two unknowns from the phase differences is obtained. So, the refraction index at the radar level and the vertical mean variation of the refraction index can be obtained [8].

III. GB-SAR DATA FOR ATMOSPHERIC REFRACTION INDEX RETRIEVAL

In this section, the Ground-Based Synthetic Aperture Radar (GB-SAR) [9] used to get the radar data to be compared with meteorological acquisitions is presented. A GB-SAR is a radar-based remote sensing system mounted in a terrestrial station to get local images. The main advantages of these systems are the spatial portability and the short temporal revisit time. So, by using a GB-SAR system, continuous images every few minutes of an area of few kilometres (1-10 km x 1-10 km) can be obtained.

A GB-SAR system consists of a moving radar payload mounted in a rail. The radar transmits and receives pulses in different positions along the rail. The different echoes coming from each target while the transmitting antenna footprint illuminates the scene are recorded and coherently processed. This technique is known as synthetic aperture radar (SAR) [10]. With SAR acquisition, using a small antenna, high resolution images are obtained by coherently processing the echoes received in the different position along the radar track. Thus, it is equivalent to have several antennas separated along the transmitter path simultaneously illuminating the scene (synthetic aperture antenna). Better and non-distance dependant azimuth resolution is achieved [10].

The data used in this analysis comes from a GB-SAR system working at X-Band (9.65 GHz). The radar moves along a baseline of 2.2 m and takes periodic images over a fixed scene. Each campaign lasts for several hours, so the temporal behaviour of the phase received from the scene target can be monitored and compared with meteorological data which is the aim of this study. Two different datasets have been considered in this analysis corresponding to Canillo (Andorra) and Montserrat (Catalonia). A sample image of each campaign is shown in Fig.(1).

IV. DATA ANALYSIS AND RESULTS

A. GB-SAR signal phase estimation from meteorological data.

Canillo dataset from 7th April 2011 has been used to see the correspondence between the phase variations and meteorological observations. The values of temperature and relative humidity can be seen in Fig.(2). The atmospheric pressure at the radar height has been estimated from 6 hours series from Wetterzentrale CFS-Reanalysis-Karten [11].

From the meteorological measurements, the phase variations expected for the received GB-SAR data have been computed and compared with the actual phase variations obtained from the GB-SAR acquisition. A single stable target within the scene has been considered to get the SAR signal phase. One of the limitations of the data considered is the absence of controlled targets, so it is not possible to control the intrinsic phase of the targets in the scene which can result in phase distortions in the estimation.
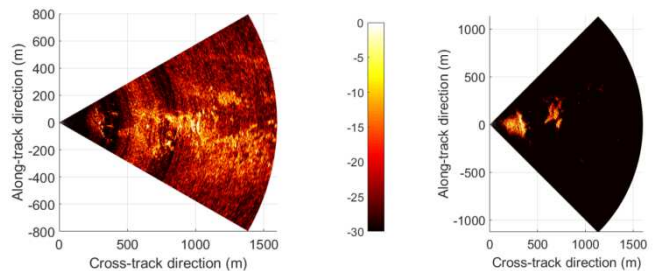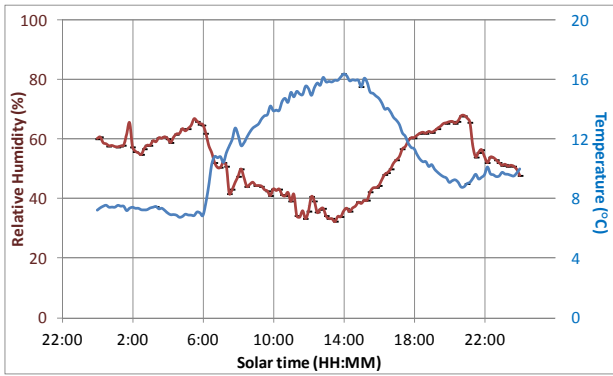

FIG. 1: Amplitude [dB] images from the Canillo (left) and Montserrat (right) campaigns. Source: UPC GB-SAR.

FIG. 2: Temperature in ℃ (±0.001℃) and R.H. in % (±0.1 %) from the station in Bony de les Neres (Comú de Canillo). Source: CENMA/IAE.

Additionally, not knowing the actual phase history of the target considered makes not possible to perform an absolute calibration of the data received. Then, only the relative changes along the acquisition can be retrieved but not the absolute phase value. The results obtained are shown in Fig.(3). As seen, the estimated phase from meteorological measurements follow the same trend than the phase measured directly with the GB-SAR data. To account for the intrinsic phase variation, a 5% error of the phase received from the GB-SAR data is considered in Fig.(3). The error for the phase estimated from meteorological data has been obtained with
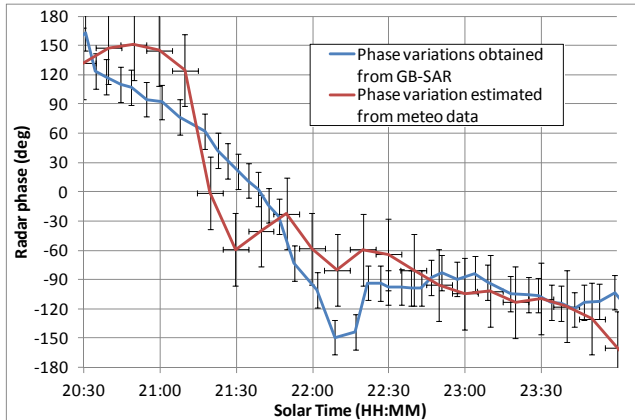
FIG. 3: Actual phase of GB-SAR data vs. estimation from meteorological data in Canillo at 7ᵗʰ April, 2011.
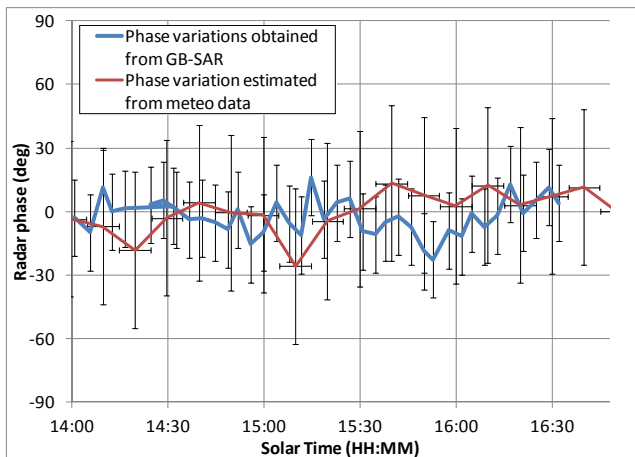
FIG. 4: Actual phase of GB-SAR data vs. estimation from meteorological data in Canillo at 9ᵗʰ June, 2011.

error propagation from the input data precision. The same analysis has been performed for another dataset collected in Canillo (Andorra) at 9ᵗʰ of June, 2011. The results obtained are shown in Fig.(4).

In both acquisitions, the phase estimation from meteorological data is close to the actual phase received from the GB-SAR. The mismatches observed can be related to different factors. First and foremost, the acquisitions considered were not intended for the atmospheric analysis. Thus, there was not any stable point in the scene at the same height than the radar location, so vertical structure of the troposphere can degrade our phase estimation. Additionally, the target considered in the estimation is a natural target, so its intrinsic phase is overlapped to the actual atmospheric variations and can not be distinguished. The results would improve by considering trihedral structures whose phase and amplitude behaviour is well known. Furthermore, these structures would allow to perform the absolute calibration. On the other hand, the meteorological data used in the analysis is from a near station, but the actual data over the scene is not available. Using the data of a near meteorological station is a good approximation to get the general trend, but local changes in temperature and humidity over the scene are not traceable and, therefore, this information is lost. Finally, having a grid of stable points spread within the scene could improve our results by interpolating the phase information.

B. Estimation of meteorological data from GB-SAR phase measurements.

Alternatively, the radar phase data can be used to retrieve meteorological information. In this section, the radar data from a Montserrat GB-SAR campaign are used to estimate the relative humidity. As in the previous section, the temperature and pressure data have been obtained from meteorological measurements and, additionally, the phase history from a stable target within the scene has been considered. The atmospheric water vapour pressure can be easily found from these input data as

$$e = \frac{T^2}{3.73 \cdot 10^5}\left(N - 77.6\frac{P}{T}\right) \qquad (14)$$

where refractivity (*N*) is related to atmospheric changes using equations (2) and (3) and the R.H. can be computed with (5).
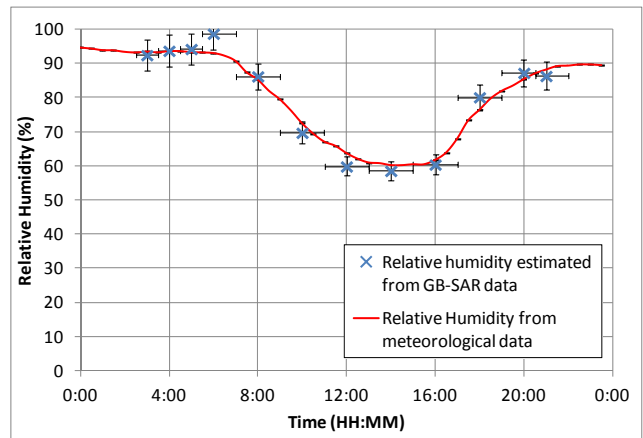
FIG. 5: R.H. estimated from the GB-SAR phase data from Montserrat vs. meteorological data at 2ⁿᵈ October 2014.

The campaign analysed consists on a 1-2 hours spaced series of acquisition at the 2nd of October 2014. The results are shown in Fig.(5) where the R.H. from meteorological acquisition is compared with the one estimated from the pressure, temperature and GB-SAR phase.

The R.H. estimation reproduces reasonably well quantitative observations and very well the daily trend of measurements from the station. Once again, the mismatches observed can be related to the causes already explained for the previous dataset but, additionally, the temporal sampling is not enough in this case. Having acquisition every 1 or 2 hours, might be too much time to get an accurate estimation of the meteorological data.

V.   CONCLUSIONS

In this analysis, the impact of the atmospheric changes on radar acquisitions is demonstrated. This phenomenon, which is seen as a perturbation in radar acquisition, can be exploited to get relevant information about the atmospheric conditions.

Two main applications have been described in this article. On one hand, the meteorological data can be used in radar acquisitions to estimate the phase variations related to atmosphere and compensate them in order to avoid defocusing problems of the image. It can be specially relevant for long integration time systems, such as recently studied GEOSAR [12]. On the other hand, this technique can be also interesting for meteorological purposes since meteorological data can be retrieved from the phase measurements obtained in a radar acquisition.

As already pointed out in the results, the data used for the analysis present some limitations such as poor temporal sampling, absence of true stable targets and lack of meteorological data in the scene location. Therefore, an ad-hoc campaign to demonstrate the feasibility of this technique to retrieve the radar phase history or to get meteorological data shall be necessary. In this case, controlled reference targets should be placed all along the scene and the meteorological data should be taken in the scene location, preferably in different height to analyse the vertical structure of the troposphere. Frequent images, every 5-10 minutes, should also be necessary.

In conclusion, this analysis is a first step to demonstrate the relation between meteorological and radar phase data. Further analysis and campaigns should be necessary to fully characterize this relation and overcome the stated limitations of the current analysis.

_____

[1] R. B. Dybdal, "Radar cross section measurements," in Proceedings of the IEEE, vol. 75, no. 4, pp. 498-516, April 1987.

[2] F. Fabry et al., "Extraction of near-surface index of refraction using radar phase measurements from ground targets," Antennas and Propagation Society International Symposium, 1997. IEEE., 1997 Digest, Montreal, Canada, 1997, pp. 2625-2628 vol.4.

[3] F. Bovenga et al. "Frequency coherent vs. temporally coherent targets," Geoscience and Remote Sensing Symposium (IGARSS), 2013 IEEE International, Melbourne, VIC, 2013, pp. 105-108.

[4] M. W. Long and M. S. Greco, "Sea and ground radar clutter modeling," Radar Conference, 2008. RADAR '08. IEEE, Rome, 2008, pp. 1-1.

[5] R. S. Raven, "Requirements on master oscillators for coherent radar," in Proceedings of the IEEE, vol. 54, no. 2, pp. 237-243, Feb. 1966.

[6] H. Lim et al., "Two new practical methods for phase unwrapping," IGARSS '95. 'Quantitative Remote Sensing for Science and Applications', International, Firenze, 1995, pp. 196-198 vol.1.

[7] B. S. Majani, "Analysis of External Drift Kriging Algorithm with application to precipitation estimation in complex orography.", Thesis from ITC Enschede, the Netherlands, January 2007.

[8] F. Fabry, "Meteorological Value of Ground Target Measurements by Radar," Journal of Atmospheric and Oceanic Tech., vol. 21, pp. 560-573, Apr. 2004.

[9] R. Iglesias et al., "Ground-Based Polarimetric SAR Interferometry for the Monitoring of Terrain Displacement Phenomena–Part I: Theoretical Description," in IEEE Journal of Selected Topics in Applied Earth Observations and Remote Sensing, vol. 8, no. 3, pp. 980-993, March 2015.

[10] J.C. Curlander and R.N. McDonough, 'Synthetic Aperture Radar: Systems and Signal Processing', Chapter 1: Introduction to SAR, New York, 1991.

[11] Wetter Zentrale. CFS Reanalysis: Informationen. http://www.wetterzentrale.de/topkarten

[12] J. Ruiz et al., "Geosynchronous SAR Focusing With Atmospheric Phase Screen Retrieval and Compensation," in IEEE Transactions on Geoscience and Remote Sensing, vol. 51, no. 8, pp. 4397-4404, Aug. 2013.